Game theory and physics

Christoph Hauert[a)]
Departments of Mathematics and Zoology, University of British Columbia, 6270 University Boulevard, Vancouver, British Columbia, Canada, V6T 1Z4

György Szabó[b)]
Research Institute for Technical Physics and Materials Science, P. O. Box 49, H-1525 Budapest, Hungary

Evolutionary game theory is designed to capture the essentials of the characteristic interactions among individuals. Its most prominent application is the quest for the origins and evolution of cooperation. The effects of population structures on the performance of behavioral strategies became apparent only in recent years and marks the advent of an intriguing link between apparently unrelated disciplines. Evolutionary game theory in structured populations reveals critical phase transitions that fall into the universality class of directed percolation on square lattices and mean-field-type transitions on regular small world networks and random regular graphs. We employ the prisoner's dilemma to discuss new insights gained in behavioral ecology using methods from physics. © *2005 American Association of Physics Teachers.*
[DOI: 10.1119/1.1848514]

I. INTRODUCTION

The evolution of cooperation is a fundamental problem in biology because unselfish, altruistic actions apparently contradict Darwinian selection. Nevertheless, cooperation is abundant in nature ranging from microbial interactions[1] to human behavior.[2] In particular, cooperation has given rise to major transitions in the history of life.[3] Game theory[4] together with its extensions to an evolutionary context[5] has become an invaluable tool to address the evolution of cooperation. The most prominent mechanisms of cooperation are direct[6,7] and indirect[8–10] reciprocity, voluntary interactions,[11–13] and spatial structure.[14–19] All these mechanisms have one thing in common: they hinge on different forms of assortative (that is, nonrandom or conditional) interactions. Such assortment can be actively implemented through discriminating strategic behavior of the interacting individuals or passively by imposing environmental constraints such as local interactions in spatially extended systems. The dynamics that results from constraining interactions to nearest neighbors suggests new and interesting and intriguing links to physics and, in particular, to statistical mechanics.

Investigations of spatially extended systems have a long tradition in condensed matter physics. Among the most important features of spatially extended systems are the emergence of phase transitions. Their analysis can be traced back to the Ising model.[20] The application of methods developed in statistical mechanics to interactions in spatially structured populations has turned out to be very fruitful.[18] Interesting parallels between nonequilibrium phase transitions and spatial evolutionary game theory have added another dimension to the concept of universality classes.

In game theory, the prisoner's dilemma[7] is a paradigm for cooperation. The prisoner's dilemma describes the pairwise interactions of individuals with two behavioral options: the two players must simultaneously decide whether to cooperate or to defect. Cooperation yields a benefit b to the coplayer at a cost c ($b > c$). Thus, for mutual cooperation both players receive the reward $R = b - c$, but only the punishment $P = 0$ for mutual defection. If one player defects and the other cooperates, the traitor receives the temptation $T = b$, while the cooperator is left with the sucker's payoff $S = -c$. These payoffs satisfy the characteristic payoff ranking of the prisoner's dilemma: $T > R > P > S$. (In repeated interactions it is additionally required that $2R > T + S$ such that mutual cooperation has the highest return for the community.) It is easy to see that defection is the better choice irrespective of the opponent's decision. Thus, ultimately individuals end up with P instead of the preferable reward R—hence the dilemma. This unfortunate outcome represents the result of classical game theory and is called a Nash equilibrium because none of the players can increase their payoff by unilaterally changing the strategy.[21]

In evolutionary game theory an infinite population is considered with a fraction ρ cooperators and $1 - \rho$ defectors. In the mean-field approximation, that is, in well-mixed populations where individuals interact randomly, the payoffs are given by $P_C = \rho R + (1 - \rho) S = \rho b - c$ and $P_D = \rho T + (1 - \rho) P = \rho b$ for cooperators and defectors, respectively. If we assume that cooperators and defectors are "spread" according to their relative performance, that is, as compared to the average population payoff $\bar{P} = \rho P_C + (1 - \rho) P_D = \rho(b - c)$, the dynamics is determined by the replicator equation:[22]

$$\dot{\rho} = \rho(P_C - \bar{P}) = \rho(1 - \rho)(P_C - P_D). \tag{1}$$

As time passes, ρ obviously converges to zero because $P_D > P_C$, that is, cooperators vanish irrespective of their initial concentration. Thus, both classical and evolutionary game theory predict the undesired outcome of mutual defection and economic stalemate, where no one receives any benefits for the sake of reducing costs.

To overcome this dilemma, we consider spatially structured populations where individuals interact and compete only within a limited neighborhood. Such limited local inter-

actions enable cooperators to form clusters and thus individuals along the boundary can outweigh their losses against defectors by gains from interactions within the cluster. Results for different population structures and for voluntary participation in the prisoner's dilemma are discussed and related to condensed matter physics.

II. SPATIALLY STRUCTURED POPULATIONS

Spatially structured populations are modeled by confining players to lattice sites or, more generally, to the nodes of an arbitrary graph. The performance P_x of a player at site x is determined by the payoffs accumulated in its interactions with its neighbors. Occasionally a player at site x reassesses its strategy by comparing its performance to a randomly selected neighbor at site y. There are different approaches for defining the update rule of player x. For example, we could assume that player x adopts the strategy of y with a probability proportional to the difference in performance $P_y - P_x$ provided that it is positive. This approach recovers Eq. (1) in the limit of random interactions (well-mixed populations) or fully connected graphs. Unfortunately, the fact that worse performing players are never imitated together with the non-differentiability when $P_y - P_x = 0$ results in subtle difficulties. Although the equilibrium frequencies of cooperators and defectors are hardly affected, this approach affects the performance and the nature of the fluctuations—the signature of critical phase transitions.

To highlight the links between spatial game theory and condensed matter physics, we assume a transition probability given by

$$W(x \leftarrow y) = f(P_y - P_x) = [1 + \exp(-(P_y - P_x)/\kappa)]^{-1}, \tag{2}$$

where κ denotes the amount of noise. This update rule states that the strategy of a better performing player is readily adopted, whereas it is unlikely (but not impossible) to adopt the strategies of worse performing players. The parameter κ incorporates the uncertainties in the strategy adoption (originating in either the variation of payoffs or in mistakes in the decision making). In the limit $\kappa \to \infty$ all information is lost, that is, player x is unable to retrieve any information from P_y and switches to the strategy of y by tossing a coin.

At first glance, this update rule seems to be similar to Glauber dynamics[23] for the kinetic Ising model where strategies translate to spin up and down, $P_y - P_x$ relates to the change of energy when flipping the spin at x, and κ corresponds to the temperature. In Glauber dynamics the probability of a single spin flip is determined by the energy difference between the initial and the flipped states. This transition rule drives the system toward the equilibrium state for the temperature κ. However, the game theoretical approach involves several important differences. Most importantly, in Glauber dynamics the energy gain of the pair interaction is shared between neighboring spins. Consequentially, spin flips that minimize the local energy also reduce the total energy. This minimization contrasts with game theoretical agents that attempt to maximize their individual payoff regardless of the potential losses for the population as a whole. In addition, players are restrained to adopt the strategies of their neighbors and are incapable of anticipating the resulting payoffs. It follows that, unlike in Glauber dynamics, strategy changes (or spin flips) occur only along boundaries which separate domains of different strategies. Thus, in the absence of spon-
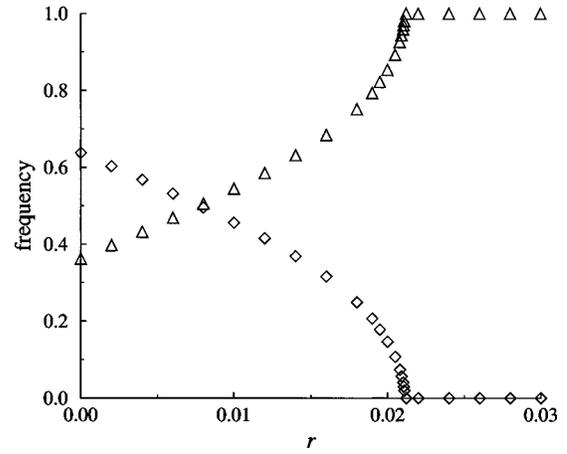

Fig. 1. Frequency of cooperators ($\diamond$) and defectors ($\triangle$) in the spatial prisoner's dilemma as a function of the cost-to-benefit ratio r. The simulations were performed on square lattices with periodic boundary conditions and population sizes ranging from $N = 400^2 = 1.6 \times 10^5$ to $N = 10^6$. In the vicinity of the extinction threshold of cooperators larger systems are used to suppress the undesired effects of diverging fluctuations.

taneous mutations, spatial games always have absorbing states where all members follow the same strategy.

The spreading of strategies resembles the spreading of infectious diseases as described by contact processes. These models exhibit (universal) nonequilibrium phase transitions (into absorbing states). Their general features are reviewed in Refs. 24 and 25.

A. Square lattices

A spatial arrangement can be approximated by considering a square lattice with periodic boundary conditions, where each individual is confined to a lattice site and interacts and competes only with its four nearest neighbors. Starting from a random initial configuration, the population is updated in an asynchronous fashion through sequential updates of randomly drawn players: first, two neighboring sites x and y are chosen at random and, second, the player at site x adopts the strategy of the player at y with the probability $W(x \leftarrow y)$ [see Eq. (2)]. After an equilibration time the system reaches a stationary state independent of the initial configuration due to the stochastic update rules. The stationary state is characterized by the density of strategies obtained by averaging over a sampling time which was varied from 10^4 to 10^6 Monte Carlo steps per site (MCS). In each MCS, every site is updated once on the average. For simplicity (but without loss of generality), the payoffs are rescaled such that $R = 1$, $T = 1 + r$, $S = -r$, and $P = 0$, where $r = c/(b - c)$ denotes the ratio of the costs of cooperation to the net benefits of cooperation.

In contrast to the results for well-mixed populations, cooperators persist at substantial levels in spatial settings if r is sufficiently small, that is, the benefits of cooperation are high compared to the costs (see Fig. 1). Cooperators survive by forming compact clusters which minimize the exploitation by defectors. Along the boundary, cooperators can outweigh their losses against defectors by gains from interactions within the cluster. A snapshot of a typical lattice configuration illustrates the clusters just below the extinction threshold
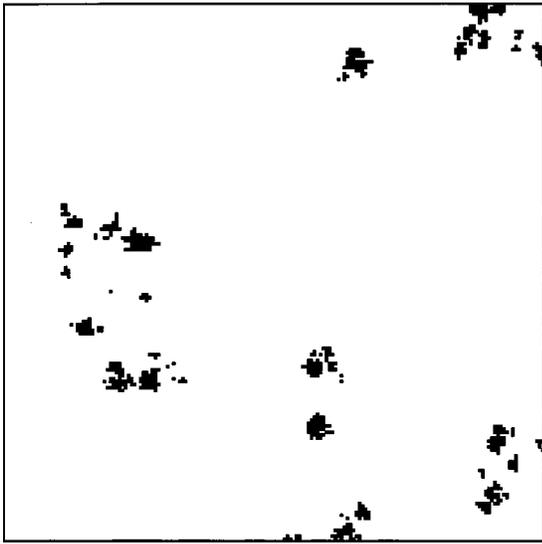
Fig. 2. Typical distribution of cooperators (black) in a sea of defectors (white) on a square lattice for $r=0.0211$ and $\kappa=0.1$, just below the extinction threshold $r_c=0.021\,12\,(2)$ of cooperators. Note that the distribution is essentially independent of the initial lattice configuration. However, in finite systems the frequency of cooperators should not be too low, so as to avoid accidental extinctions while approaching the stationary state.

Fig. 3. Log-log plot of the average fraction of cooperators ρ as a function of the distance to the extinction threshold r_c-r. The solid line shows that in the vicinity of r_c, the power law $\approx(r_c-r)^\beta$ perfectly fits the data with $r_c=0.021\,12\,(2)$ and $\beta=0.57\,(3)$. The system size was increased as r approaches r_c from $N=1.6\times10^5$ to $N=10^6$.

r_c (see Fig. 2). For $r>r_c$ cooperators vanish because the benefits of spatial clustering are no longer sufficient to offset the losses along the boundary.

In biology, such thresholds are common in the evolution of cooperative behavior. Probably the first quantitative treatment goes back to W. D. Hamilton's kin selection theory.[26] Cooperation among relatives evolves and is beneficial from a genetic point of view[27] whenever $r_{kin}>c/b$, that is, the degree of relatedness r_{kin} exceeds the cost-to-benefit ratio of cooperation. This idea is illustrated by an anecdote attributed to J. B. S. Haldane[28] who apparently claimed that he would give his life to save more than two drowning siblings or more than eight drowning cousins. The basis for this calculation is the fact that the degree of relatedness in humans (that is, the fraction of genes shared by two individuals) generally does not exceed $\frac{1}{2}$. In the present context, the threshold r_c is considerably smaller than r_{kin} (also note the slightly different definitions of r and r_{kin}), that is, persistence of cooperation requires much greater benefits from the cooperative action. One major reason for this significant reduction of feasible cost-to-benefit ratios r that are capable of maintaining cooperation is that we are considering unrelated and selfish individuals.

According to our simulations, near r_c the average fraction of cooperators vanishes as $\langle\rho\rangle\approx(r_c-r)^\beta$ (see Fig. 3) where $r_c=0.021\,12\,(2)$ and $\beta=0.57\,(3)$ (the figures between parentheses indicate the statistical uncertainties of the last digit). In these simulations the linear size of the system is chosen to be significantly larger than the correlation length and the average values are determined by averaging over a sufficiently long sampling time in the stationary state. For this purpose the linear size increased from $L=400$ to 1000, meanwhile the sampling time varied from 10^4 to 10^6 MCS when approaching the threshold r_c. Under these conditions the error bar of the MC data is less than the symbol size in Fig. 3. In physics, such thresholds r_c are usually associated
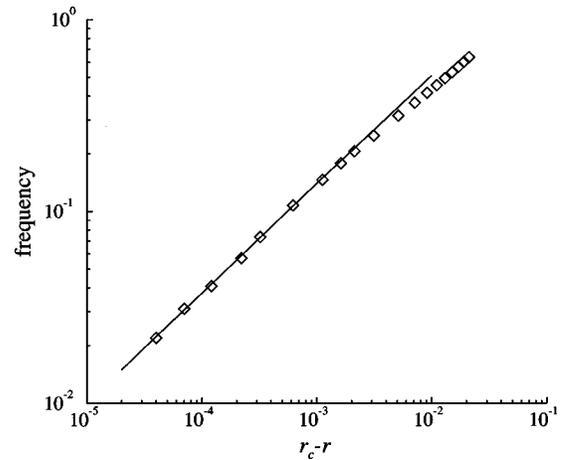
with phase transitions—and indeed, the transition from persistent levels of cooperation ($r<r_c$) to homogenous states of defection ($r>r_c$) bears the hallmarks of a critical phase transition.

On square lattices, cooperators are able to persist by forming clusters (see Fig. 2). Due to stochastic fluctuations these clusters move in a random fashion. Occasionally, a cluster splits into two or two clusters, collides, merges, or annihilates and vanishes. Territories governed by defection are only slowly invaded by clusters of cooperators because of their diffusivelike motion. For r near r_c from below, these features result in a power law divergence in the correlation length and the relaxation time, as well as in the fluctuations of the frequency of vanishing cooperators. The exponents of the different power laws characterize universal features of these nonequilibrium transitions. The extinction of cooperators falls into the directed percolation universality class.[29] Similar exponents are observed in the two-dimensional contact process that describes the spreading of epidemics or rumors,[30,31] and in branching-annihilating random walks.[32,33]

B. Random regular graphs and regular small world networks

Regular graphs are a special set of network structures where each individual has the same number of connections/links to other individuals, that is, each individual has the same connectivity. The square lattice is an example of a regular graph. In a random regular graph (RRG) the interaction partners are not limited to the immediate neighborhood but are randomly drawn from the entire population. Random regular graphs are good approximations to structured populations where spatial distances weakly affect interactions.

Small world networks have attracted considerable attention during the last few years. These networks provide a natural combination of high local connectedness and a few long-range connections that result in short average path lengths between any two nodes, ("six degrees of separation").[34] This feature is common to a wide variety of structures ranging from food webs in ecosystems and ac-
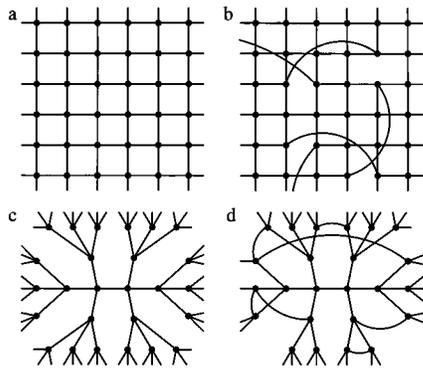
Fig. 4. Different population structures where each player or node maintains the same number of connections: (a) regular (square) lattice, (b) regular small world network (RSW), (c) Bethe lattice or tree, and (d) random regular graph (RRG). Regular small world networks are generated from regular lattices by randomly rewiring some fraction of connections constrained only by the requirement that the connectivity must be preserved. If all connections are replaced, an RRG is obtained. In that sense, (a) and (d) represent the two extremes of regular small world networks. In the limit $N \to \infty$. RRG becomes locally similar to a tree (c).[38]

quaintance networks in humans to the power grid in North America and the physical and logical structure of the world wide web.[35,36]

Small world networks can be easily generated by starting with a square lattice and then randomly rewiring a certain fraction Q of all connections by replacing local links with global ones[37] (see Fig. 4). In the following we restrict our discussion to regular small world networks (RSW), that is, to population structures where each individual keeps the same number of connections. Keeping the connectivity constant simplifies comparisons and highlights the differences due to the different spatial arrangement. The parameter Q lets us tune the structure of the network: for $Q=0$ we have a square lattice and in the limit $Q \to 1$ we obtain a random regular
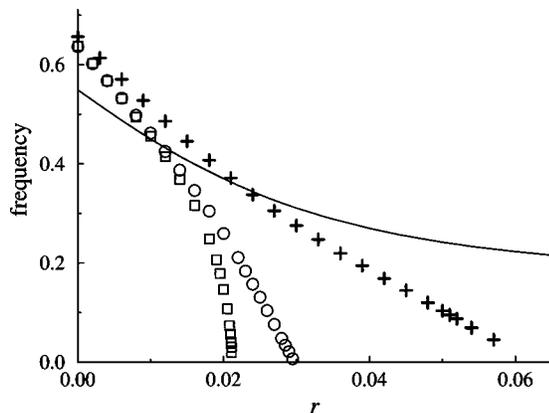
graph. For small Q typical regular small world networks are generated, preserving many short loops of square lattices, but substantially reducing the average minimal distance between any two nodes, that is, the number of links along the shortest path. The underlying population structure has significant effects on the performance of cooperators as shown in Fig. 5.

Surprisingly, it turns out that cooperators perform significantly better on random regular graphs than on square lattices. As expected, the performance of cooperators on regular small world networks lies between these two extremes. Thus, the substitution of long-range connections for local ones actually benefits cooperation. This increase in cooperation is in contrast with the naive expectation that cooperators would suffer from weakening local structures and clustering abilities. On the contrary, random regular graphs lead to better chances for cooperators as compared to regular lattices.

Another important but more subtle difference is the nature of the extinction of cooperators. On the square lattice cooperators vanish according to a power law (see Fig. 3) with the exponent $\beta=0.57$ (3), which is characteristic of all two-dimensional ($d=2$) systems. However, for the directed percolation universality class, the value of β depends on the spatial dimension d. Mean-field type transitions ($\beta=1$) occur for $d \geq 4$ (for details see Refs. 24 and 25) as well as on Bethe lattices and trees.[39] In the limit of large populations $N \to \infty$, random regular graphs become locally similar to a Bethe lattice. On small world networks, the spatial correlations are essentially destroyed by the random long-range connections. As a consequence, mean-field-type transitions occur for both random regular graphs and small world networks, that is, cooperators vanish linearly with r.

In the absence of spatial structure, that is, in well mixed populations (mean-field approximation), a discontinuous transition occurs at $r_c=0$ with full cooperation ($\rho=1$) for $r<0$ and all out defection ($\rho=0$) for $r>0$. The more sophisticated pair approximation provides an analytically accessible way to determine the corrections from spatial structure in quenched arrangements. Instead of the equilibrium frequency of strategies, the pair approximation considers the frequency of strategy pairs (see the Appendix). This improved approach correctly predicts the trends, that is, the persistence of cooperation for $r>0$ and suggests a linear decrease of the frequency of cooperators. However, it is unable to adequately describe the formation of small clusters of cooperators (see, for example, Fig. 2), and therefore it significantly overestimates the extinction threshold with $r_c^{pair}=0.290$ (1) in contrast to $r_c<0.021\,12$ (2) obtained from the simulations. In addition, the pair approximation is incapable of distinguishing the different population structures because of their identical connectivity.

The remarkable differences in the results for different spatial structures clearly indicate that cooperation is sensitive to the topological features of the underlying population structure. The variation of the results can be further extended by allowing variations in the numbers of neighbors of each individual, that is, on diluted lattices with vacant sites[40,41] or on social networks with different types of underlying structures.[42–44]

Fig. 5. Fraction of cooperators ρ as a function of r for different population structures: square lattice ($\square$), random regular graph ($+$), and regular small world networks ($\bigcirc$) for $Q=0.03$, $\kappa=0.1$, and $N=1.6\times10^5–10^6$. For increasing r, the spatial correlations result in a critical transition on the square lattice (see Fig. 3), whereas on random regular graph and small world networks the lack of correlations lead to a linear decrease in cooperation, that is, a mean-field type transition. The data referring to homogeneous D states (cooperators go extinct and defectors reach fixation) is omitted. The pair approximation (solid line) correctly predicts the trend, but significantly overestimates the benefits of population structures (see the text and the Appendix for details).
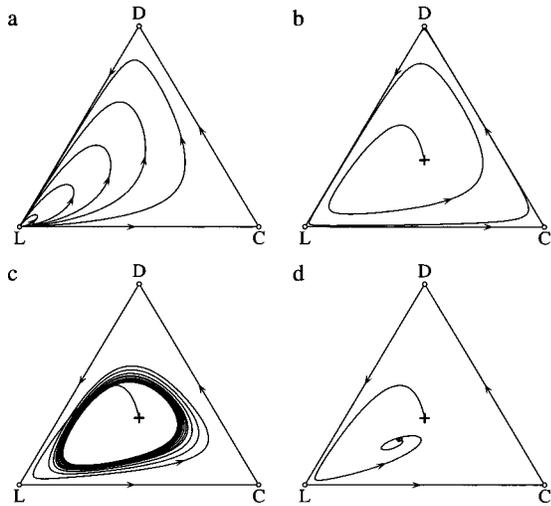
Fig. 6. Sample trajectories of the evolution of the frequencies of cooperators, defectors, and loners in the voluntary prisoner's dilemma for different population structures. The boundary of the simplex S_3 consists of a heteroclinic cycle which reflects the cyclic dominance of the three strategies. (a) In well-mixed populations the system relaxes into homogenous states of all loners. (b) For RRG the trajectories spiral outward and eventually end in one of the three absorbing states, but usually they end in the loner corner as in (a). (c) Regular small world networks networks ($Q = 0.03$) substantially change this outcome and reveal an asymptotically stable limit cycle leading to persistent global oscillations of the three strategies. (d) On square lattices the system evolves toward a stable stationary state with all three strategies coexisting [$\rho_D = 0.229$ (1), $\rho_C = 0.269$ (1), and $\rho_L = 0.502$ (1)]. All simulations [(b)–(d)] were done for the for $r = 0.4$, $\sigma = 0.3$, $\kappa = 0.1$, and $N = 10^6$. Note that for these parameters defectors invariably reach fixation (cooperators go extinct) in the absence of the loners. The simulations in (b)–(d) have random initial configurations with identical concentrations of all three strategies (marked by +).

III. VOLUNTARY PARTICIPATION

So far we have implicitly assumed compulsory participation in the prisoner's dilemma. In many situations, however, individuals often may drop out of unpromising and risky social enterprises and instead rely on the perhaps smaller but at least secure earnings based on their individual efforts. In the context of human societies, one of the pioneers to study and discuss characteristics of social interactions in a modern way was the French philosopher J. J. Rousseau.[45] He described a hunting party where each participant faced the choice of dropping out and collecting mushrooms alone or hunting hares with a partner. An individual might be better off collecting mushrooms than relying on the efforts of an undependable partner. However, by doing so individuals forfeit their chances of catching the larger, more favorable game but also avoid the risk of facing an empty plate for dinner. Note that defectors also threaten the success of the common enterprise but for different reasons: defectors portray opportunistic participants that attempt to free ride on the efforts of the community, that is, they are hoping for a free lunch.

In game theoretical terms the payoff of risk-averse loners is constant $P_l = \sigma$ with $P = 0 < \sigma < R = 1$, that is, loners are better off than a pair of defectors, but fare less well than two cooperators. If one of the two individuals chooses the loner option, the other individual is forced to act as a loner. The three strategies of cooperation, defection, and going it alone implements a rock-scissors-paper-type cyclic dominance: if participants are likely to cooperate, it pays to defect; how-
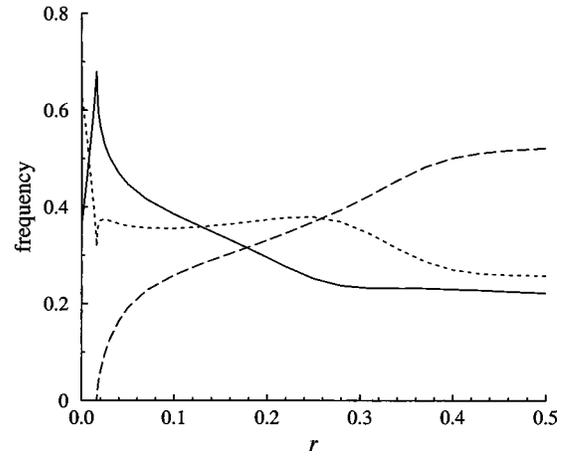

Fig. 7. The average fraction of cooperators (dotted line), defectors (solid line), and loners (dashed line) as a function of the cost-to-benefit ratio r on square lattices for $\sigma = 0.3$, $\kappa = 0.1$, and $N = 1.6 \times 10^5 - 10^6$. For $r < r_{c1}^{(sq)} = 0.016$ (1) loners go extinct because cooperators thrive on their own, but for all other r the three strategies coexist in dynamical equilibrium [see Fig. 6(d).

ever, if everybody defects, it is better to drop out, and once the loners have conquered the defector's threat, the benefits of cooperation become attractive again.

It turns out that in unstructured, well mixed populations, cooperative behavior vanishes and invariably the absorbing homogenous state with all loners occurs [see Fig. (6a)].[46]

Although loners provide an escape hatch out of states of mutual defection, this mechanism is capable of promoting persistent cooperative behavior only in larger groups of interacting individuals.[11] For pairwise interactions, the resulting advantage is insufficient and social interactions disappear. The cyclic dominance of the three strategies is reflected in the heteroclinic cycle (a closed trajectory that contains fixed points) along the boundary of the simplex S_3 (ternary phase diagram with $\rho_D + \rho_C + \rho_L = 1$). This outcome changes completely when spatial structure and local clustering are introduced [see Figs. 6(b)–6(d)]. Although random regular graphs produce only some transient fluctuations in the strategy concentrations and (usually) continue to relax in a state of all loners, regular small world networks may lead to persistent periodic oscillations of all three strategies.

A. Square lattices

In Sec. II we demonstrated that for compulsory interactions, cooperative behavior persists in spatially structured populations provided that the benefits of cooperation are sufficiently high, that is, $r < r_c$. Relaxing the compulsory interactions and allowing for voluntary participation boosts cooperation on square lattices. In fact, the loners option enables cooperators to survive for all r (see Fig. 7), which is in contrast to the compulsory prisoner's dilemma where cooperators go extinct for $r > r_c$ (see, for example, Fig. 1).

Two different dynamical regimes can be identified depending on r: For $r < r_{c1}^{(sq)}$, that is, large benefits and small costs, loners vanish because they no longer provide a viable alternative and the spatial clustering enables cooperators to survive on their own (see Fig. 2). Interestingly, the dynamics eliminates the voluntary interactions and restores the compulsory interactions characterizing the traditional prisoner's
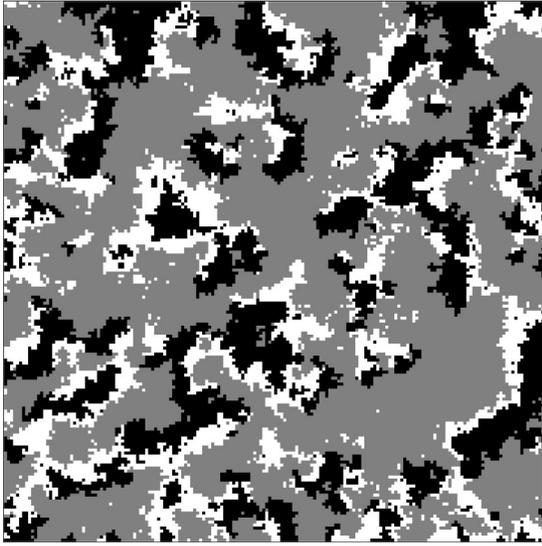
Fig. 8. Snapshot of a typical lattice configuration where cooperators (black), defectors (white), and loners (gray) coexist in dynamical equilibrium (r = 0.4, σ = 0.3, and κ = 0.1). The cyclic dominance of the three strategies promotes and maintains coexistence and leads to self-organizing patterns: each domain invades other domains of the inferior strategy while being invaded by domains of the superior strategy. Note that this distribution is independent of the initial lattice configuration, but note that in finite systems all initial frequencies should be sufficiently high to prevent accidental extinctions while approaching the stationary state.
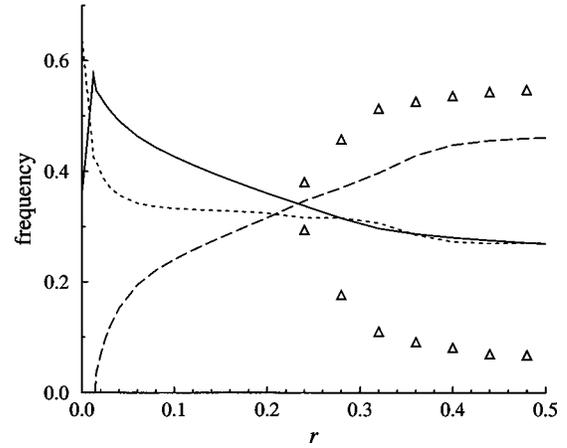

Fig. 9. The average fraction of cooperators (dotted line), defectors (solid line), and loners (dashed line) as a function of the cost-to-benefit ratio r on regular small world networks (Q = 0.03, σ = 0.3, κ = 0.1, N = 1.6 $\times 10^5 - 10^6$). There are three dynamical regimes: Loners go extinct for $r < r_{c1}^{(RSW)} = 0.015$ (1) because cooperators thrive on their own through cluster formation. For $r_{c1}^{(RSW)} < r < r_{c2}^{(RSW)} = 0.24$ (2) all three strategies coexist in a stationary state. Finally, for $r > r_{c2}^{(RSW)}$ global synchronization occurs as indicated by the maximum and minimum frequency of defectors ($\triangle$) along the limit cycle [see Fig. 6(c)].

dilemma. For more hostile settings for cooperation, that is, for $r > r_{c1}^{(sq)}$, loners are of vital importance and manage to ensure the persistence of cooperation even under harsh conditions when $r \to 1$. In this case all three strategies coexist in dynamical equilibrium.

The extinction of loners again belongs to the directed percolation universality class.[47] At first glance this affiliation might seem surprising because in the previous examples the absorbing state was a static configuration with all defectors, but here coexisting cooperators and defectors form a fluctuating background. Theory supports the idea that (on large length scales) the characteristic features of directed percolation transitions remain unaffected by temporal fluctuations of the background.[25]

Loners survive by relentlessly invading adjacent territories occupied by defectors while being diminished by succeeding cooperators. Consequently, loners die out once the defector's density becomes too low for sufficiently small r. For higher r, loners thrive on defectors, but are kept in check by cooperators as dictated by the cyclic dominance of the three strategies. The cyclic dominance results in fascinating self-organizing, spatio-temporal patterns (see Fig. 8).[48]

The cyclic invasions stabilize the coexistence of all three strategies. In particular, they maintain substantial levels of cooperation for essentially the entire range of r. This surprising robustness is a direct consequence of the system's unusual response to external effects: if a strategy is externally supported (for example, by adjusting the parameters), then not the strategy but its "predator," that is, the superior strategy benefits from the change. For this reason the frequency of loners increases with r (larger r favors defection because cooperation is less beneficial). Similar mechanisms have been reported for several systems including the maintenance of biodiversity in bacterial colonies.[49-51]

B. Regular random graphs and small worlds

For a small fraction of long-range connections Q, regular small world networks essentially preserve the local structure of the square lattice and add only a few long-range connections. Therefore, it is not surprising that the average frequencies of the strategies is barely affected (compare Fig. 9 with the square lattice results in Fig. 7).

As before, for $r < r_{c1}^{(RSW)} = 0.015$ (1) (Q = 0.03) loners become extinct and clusters of cooperators survive in a sea of defectors. In contrast, for $r > r_{c1}^{(RSW)}$ all three strategies coexist. However, on close inspection, it turns out that for
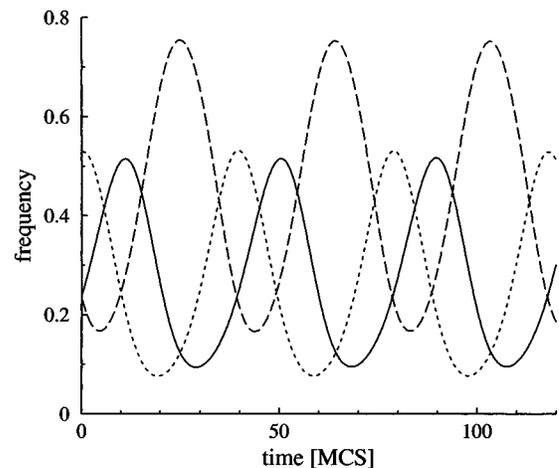

Fig. 10. The evolution of the frequencies of cooperators (dotted line), defectors (solid line), and loners (dashed line) on regular small world networks (Q = 0.03, r = 0.4, σ = 0.3, κ = 0.1, N = 10^6). The few long-range connections are sufficient to achieve global synchronization. The succession of maxima (minima) again reflects the cyclic dominance of the three strategies [see Fig. 6(c)].
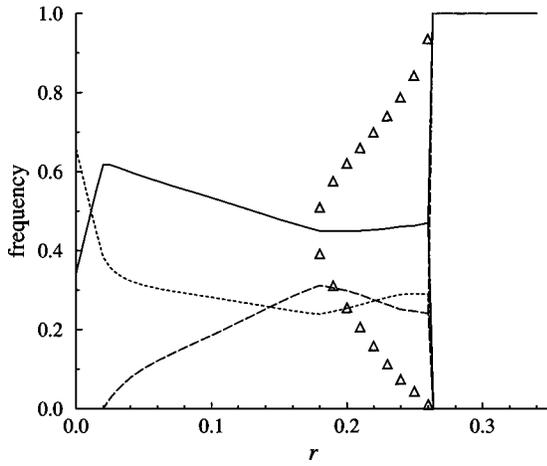
Fig. 11. The average fraction of cooperators (dotted line), defectors (solid line), and loners (dashed line) as a function of r on RRG ($\sigma = 0.3$, $\kappa = 0.1$, $N = 5 \times 10^5$). There are four dynamical regimes: Loners go extinct for $r < r_{c1}^{(RRG)} = 0.020$ (1), for $r_{c1}^{(RRG)} < r < r_{c2}^{(RRG)} = 0.180$ (5) all three strategies coexist in a stationary state. For $r_{c2}^{(RRG)} < r < r_{c3}^{(RRG)} = 0.263$ (3) the strategy frequencies oscillate periodically, and for $r > r_{c3}^{(RRG)}$, the amplitude of the oscillations increases until one strategy goes extinct and subsequently the system reaches a homogenous absorbing state. Persistent oscillations are indicated by the maximum and minimum values of ρ_D ($\triangle$).
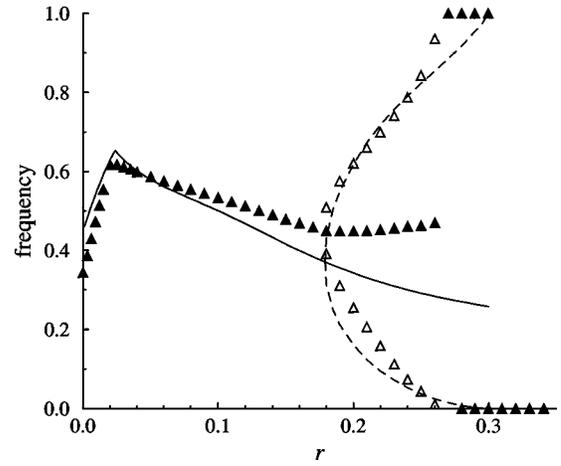

Fig. 12. The average frequency of defectors ($\blacktriangle$) on RRG together with predictions of the pair approximation (solid line) ($\sigma = 0.3$, $\kappa = 0.1$, $N = 5 \times 10^5$). In the regime of global oscillations, the maximum and minimum frequencies of defectors along the limit cycle are indicated by simulations ($\triangle$) and the pair approximation (dashed line). For $r > 0.298$ (2) the pair approximation predicts spiral trajectories converging toward the boundary of the simplex S_3.

$r > r_{c2}^{(RSW)} = 0.24$ (2) ($Q = 0.03$) persistent global periodic oscillations occur. This behavior is illustrated in Fig. 10 and indicated in Fig. 9 by the minimal and maximal defector frequencies.

Thus, the structural disorder introduced by random long-range connections can induce global synchronization. In contrast, on square lattices each site typically alternates its strategy in cycles, but the limited nearest neighbor interactions are unable to synchronize these local oscillations on a global scale.

Naturally, the onset and amplitude of global oscillations depends on Q. For example, the amplitude increases with Q until eventually a threshold is reached where the oscillations become big enough such that one strategy goes extinct and inevitably a second strategy follows (because of the cyclic dominance), leaving the system in a homogenous absorbing state. In the limit $Q \to 1$, that is, on the random regular graph, the results are illustrated in Fig. 11.

The cost-to-benefit ratio r distinguishes four dynamical regimes: For $r < r_{c1}^{(RRG)} = 0.020$ (1) cooperators and defectors coexist while loners go extinct. For $r_{c1}^{(RRG)} < r < r_{c2}^{(RRG)} = 0.180$ (5), the three strategies reach a stationary state with vanishing fluctuations (in the limit $N \to \infty$). Note that when approaching $r_{c1}^{(RRG)}$ from above, the frequency of loners vanishes linearly, $\rho_L \propto (r - r_{c1})$. Above $r_{c2}^{(RRG)}$, global synchronization kicks in, which leads to global oscillations of the strategy frequencies. For $r_{c2}^{(RRG)} < r < r_{c3}^{(RRG)} = 0.263$ (3), the oscillations are bounded as indicated by the maxima and minima of $\rho_D(t)$ in Fig. 11. (The threshold $r_{c3}^{(RRG)}$ is obtained by linear extrapolation of the maximal/minimal defector frequencies.) Note that these oscillations persist and do not decrease and converge to the corresponding average in the limit $N \to \infty$. The amplitude of the oscillations increases with r such that for $r > r_{c3}^{(RRG)}$, one strategy eventually vanishes— inevitably followed by the extinction of a second strategy— and the system reaches a homogenous absorbing state.[52] The

three basins of attraction, that is, the probabilities to end up with only cooperators, defectors, or loners, depend on the parameters r, σ, and κ. A state of all loners is the most likely outcome for large r and Q as found in well mixed populations.

Even though the predictive power of the pair approximation turns out to be rather limited in the compulsory prisoner's dilemma, the results for the voluntary prisoner's dilemma are in very good agreement with simulations on random regular graphs. Figure 12 illustrates that not only the frequency of defectors is well reproduced, but also the onset and the amplitude of global oscillations.

IV. SUMMARY AND CONCLUSIONS

The effects of population structure turn out to be essential for the evolution of cooperation. The spatial extension of lattices or the rigid arrangement of individuals on regular small world networks and random regular graphs enables cooperators to thrive through cluster formation. In this way cooperators offset losses against defectors with gains from fellow cooperators. In contrast, in well mixed populations cooperators are doomed and defectors reign. However, the advantages arising through population structures are rather limited, that is, in the compulsory prisoner's dilemma interactions very favorable cost-to-benefit ratios r are required (the benefits must exceed costs by a factor of 20). This situation changes drastically when voluntary participation is added by introducing the loner strategy, that is, the option to not participate in the social enterprise. In well mixed populations the risk averse loners reign, but on square lattices cooperators persist for all r. On regular small world networks and random regular graphs, the range of r viable for cooperators is greatly enhanced. Only for very small r do loners become extinct, that is, the system's dynamics reverts voluntary participation back into compulsory interactions. For larger r, the long-range connections in regular small world networks and random regular graphs promote global synchronization and lead to global periodic oscillations of
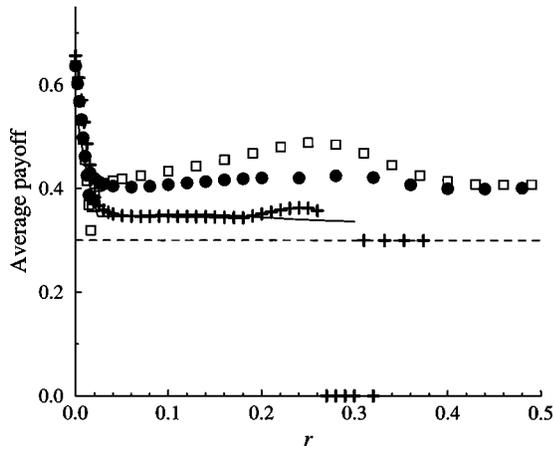
Fig. 13. The average population payoff in the voluntary prisoner's dilemma as a function of r for different population structures: square lattice ($\square$), RRG ($+$), and regular small world networks ($\bullet$) with $Q=0.03$, $\sigma=0.3$, $\kappa=0.1$ and $N=1.6\times10^5-10^6$ together with predictions from the pair approximation (solid line). For comparison, the average performance of well-mixed populations (dashed line) is shown, which amounts to the loners payoff σ. In structured populations the payoff lies significantly above σ [with the exception of $r>r_{c3}^{(\text{RRG})}=0.263$ (3), where increasing oscillations again favor homogenous states with all loners], but nevertheless quite a bit below $R=1$ for mutual cooperation. Thus, population structure is capable of at least partly resolving the dilemma of cooperation.

the strategy frequencies. The amplitude of this limit cycle increases with r as well as with the fraction of rewired connections on regular small world networks and eventually may lead to the extinction of either strategy. The cyclic dominance of cooperators, defectors, and loners dictates that inevitably a second strategy is doomed, leaving a homogenous absorbing state behind. The basin of attraction for the three absorbing states depends on the parameter values but usually loners survive as in the well mixed scenario.

From an evolutionary perspective, not only is the persistence/abundance of cooperation of immediate interest, but also the individuals' performance, that is, their payoffs. In the compulsory game and in the absence of cooperation the payoff is clearly zero, but below the threshold where cooperators survive, the average population payoff increases to 0.635 (1) on the square lattice and 0.654 (1) on random regular graphs in the limit $r\rightarrow0$ for $\sigma=0.3$ and $\kappa=0.1$. These payoffs are still less than the maximum return for mutual cooperation with $R=1$ for mutual cooperation, but at least the population structure is capable of resolving part of the dilemma. In the voluntary prisoner's dilemma in well mixed populations everybody obviously earns the loner's payoff σ. But in structured populations everybody is again better off—at least on average (see Fig. 13). Interestingly, the average payoff of cooperators is substantially higher than that of defectors, but, nevertheless, the prospects and temptation of short term profits limits the extent of cooperative behavior. As in the compulsory prisoner's dilemma, structured populations, that is, fixed partnerships, partially resolve the dilemma and improve social welfare.

The insights into the evolution of cooperation would not be possible without the fruitful applications of methods and techniques developed in statistical and condensed matter physics, in particular, the concept of phase transitions and universality classes. Intriguing and fruitful interdisciplinary links between physics, biology, and the social sciences are
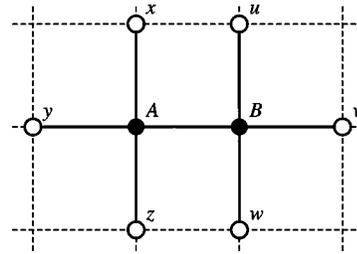
emerging,[53] but the future prospects of such collaborations depend on behavioral scientists embracing mathematical concepts as well as physicists adjusting their theoretical framework to the conditions and requirements arising in the dynamics of living systems.

Fig. 14. Small part of square lattice indicating the relevant configuration for the pair approximation with sites A and B. This configuration is used to determine changes in the pair configuration probabilities $p_{A,B\rightarrow B,B}$. The fact that x, u and z, w are neighbors is neglected by the pair approximation, that is, it does not take into account corrections arising from loops. For this reason, the pair approximation is unable to distinguish between square lattices, regular small world networks, and RRG with identical connectivities.

APPENDIX: PAIR APPROXIMATION IN GAME THEORY

An analytical approximation of the spatial dynamics can be obtained using the pair approximation. Instead of considering the frequency of strategies as in well mixed populations, that is, in mean-field theory, the pair approximation tracks the frequencies of strategy pairs. Such pair configurations $p_{s,s'}$ indicate the probability of finding an individual playing strategy s accompanied by a neighbor playing s'. In principle, s,s' may refer to members of an arbitrary finite set of strategies. However, to keep the formulas simple, we consider cooperators C and defectors D only. It is straightforward but tedious to include a third strategy such as loners.[47,54]

The pair approximation is based on three conditions: compatibility, symmetry, and closure. Consistency and compatibility in mean-field theory requires that $p_s=\Sigma_{s'}p_{s,s'}$, where p_s denotes the frequency of s and the sum runs over the set of all strategies under consideration. For two strategies this condition yields the symmetry $p_{s,s'}=p_{s',s}$. In general, this symmetry does not follow from the compatibility requirements,[55] but can be assumed for stochastic update rules. Finally and most importantly, configuration probabilities of larger clusters are approximated by pair configuration probabilities—this approximation is known as closure. For example, the configuration probability of a three site cluster s,s',s'' is approximated by $p_{s,s',s''}=p_{s,s'}p_{s',s''}/p_{s'}$, where the denominator corrects for the fact that both $p_{s,s'}$ and $p_{s',s''}$ include the probability for s'.

In spatially structured populations, the strategy of a randomly chosen site A is updated by comparing its performance to a randomly chosen neighbor B. Figure 14 illustrates this situation for a square lattice with four neighbors.

The payoffs P_A and P_B of A and B are determined by accumulating the payoffs in interactions with their neighbors x, y, z, B and u, v, w, A, respectively. The pair approxi-

mation is completed by determining the evolution of the pair configuration probabilities, that is, the probability that the pair $p_{A,B}$ becomes $p_{B,B}$:

$$p_{A,B\to B,B} = \sum_{x,y,z} \sum_{u,v,w} f(P_B - P_A)$$

$$\times \frac{p_{x,A}p_{y,A}p_{z,A} \; p_{A,B}p_{u,B} \; p_{v,B}p_{w,B}}{p_A^3 p_B^3}, \quad \text{(A1)}$$

where the transition probability $f(P_B - P_A)$ [see Eq. (2)] is multiplied by the configuration probability and summed over all possible configurations. If B succeeds in populating site A, the pair configuration probabilities change: the probabilities $p_{B,B}$, $p_{B,x}$, $p_{B,y}$, and $p_{B,z}$ increase, while the probabilities $p_{A,B}$, $p_{A,x}$, $p_{A,y}$, and $p_{A,z}$ decrease. These changes result in a set of ordinary differential equations:

$$\dot{p}_{c,c} = \sum_{x,y,z} [n_c(x,y,z)+1]p_{d,x}p_{d,y}p_{d,z} \sum_{u,v,w} p_{c,u}p_{c,v}p_{c,w} f(P_c(u,v,w) - P_d(x,y,z))$$

$$- \sum_{x,y,z} n_c(x,y,z)p_{c,x}p_{c,y}p_{c,z} \sum_{u,v,w} p_{d,u}p_{d,v}p_{d,w} f(P_d(u,v,w) - P_c(x,y,z)), \quad \text{(A2a)}$$

$$\dot{p}_{c,d} = \sum_{x,y,z} [1 - n_c(x,y,z)]p_{d,x}p_{d,y}p_{d,z} \sum_{u,v,w} p_{c,u}p_{c,v}p_{c,w} f(P_c(u,v,w) - P_d(x,y,z))$$

$$- \sum_{x,y,z} [2 - n_c(x,y,z)]p_{c,x}p_{c,y}p_{c,z} \sum_{u,v,w} p_{d,u}p_{d,v}p_{d,w} f(P_d(u,v,w) - P_c(x,y,z)), \quad \text{(A2b)}$$

where $n_c(x,y,z)$ is the number of cooperators among the neighbors x, y, z, and $P_c(x,y,z)$ and $P_d(x,y,z)$ specify the payoffs of a cooperator (defector) interacting with the neighbors x, y, z plus a defector (cooperator). Note that these two differential equations are sufficient because of the symmetry condition $p_{c,d} = p_{d,c}$ and the obvious constraint $p_{c,c} + p_{c,d} + p_{d,c} + p_{d,d} = 1$. (Including the loner strategy leads to a set of nine ordinary differential equations, but symmetry conditions and constraints reduce the set to five equations.) For simplicity, Eq. (A2) omits the common factor $2p_{c,d}/(p_c^3 p_d^3)$, which corresponds to a nonlinear transformation of the time scale but leaves equilibrium unaffected. The equilibrium values $\hat{p}_{s,s'}$ are obtained either by numerical integration or by setting $\dot{p}_{c,c} = \dot{p}_{c,d} = 0$ and solving for $p_{c,c}$ and $p_{c,d}$. The $\hat{p}_{s,s'}$ then return an approximation of the equilibrium frequencies $\hat{p}_s = \Sigma_{s'} \hat{p}_{s,s'}$.

Generally, predictions by the pair approximation are less reliable near the extinction thresholds, because this approximation does not account for corrections arising from loops nor the long range correlations occurring in the vicinity of critical transitions. The accuracy of this technique can be improved by considering configuration probabilities of larger clusters. The improvement may not only be quantitative,[18] but in some cases even qualitative.[56]

[a] Current address: Program for Evolutionary Dynamics, Harvard University, One Brattle Square, Cambridge, MA, 02138. Electronic mail: christoph_hauert@harvard.edu; hauert@zoology.ubc.ca

[b] Author to whom correspondence should be addressed. Electronic mail: szabo@mfa.kfki.hu

[1] P. E. Turner and L. Chao, "Escape from prisoner's dilemma in RNA phage Φ6," Am. Nat. **161**, 497–505 (2003).

[2] A. M. Colman, *Game Theory and its Applications in the Social and Biological Sciences* (Butterworth-Heinemann, Oxford, 1995).

[3] J. Maynard Smith and E. Szathmáry, *The Major Transitions in Evolution* (Freeman, Oxford, 1995).

[4] J. von Neumann and O. Morgenstern, *Theory of Games and Economic Behaviour* (Princeton U. P., Princeton, 1944).

[5] J. Maynard Smith and G. Price, "The logic of animal conflict," Nature (London) **246**, 15–18 (1973).

[6] R. L. Trivers, "The evolution of reciprocal altruism," Q. Rev. Biol. **46**, 35–57 (1971).

[7] R. Axelrod, *The Evolution of Cooperation* (Basic Books, New York, 1984).

[8] R. D. Alexander, *The Biology of Moral Systems* (Aldine de Gruyter, New York, 1987).

[9] M. A. Nowak and K. Sigmund, "Evolution of indirect reciprocity by image scoring," Nature (London) **393**, 573–577 (1998).

[10] C. Wedekind and M. Milinski, "Cooperation through image scoring in humans," Science **288**, 850–852 (2000).

[11] C. Hauert, S. De Monte, J. Hofbauer, and K. Sigmund, "Volunteering as red queen mechanism for cooperation in public goods games," Science **296**, 1129–1132 (2002).

[12] G. Szabó and C. Hauert, "Phase transitions and volunteering in spatial public goods games," Phys. Rev. Lett. **89**, 118101-1–4 (2002).

[13] D. Semmann, H. J. Krambeck, and M. Milinski, "Volunteering leads to rock-paper-scissors dynamics in a public goods game," Nature (London) **425**, 390–393 (2003).

[14] M. A. Nowak and R. M. May, "Evolutionary games and spatial chaos," Nature (London) **359**, 826–829 (1992).

[15] A. V. M. Herz, "Collective phenomena in spatially extended evolutionary games," J. Theor. Biol. **169**, 65–87 (1994).

[16] K. Lindgren and M. G. Nordahl, "Evolutionary dynamics of spatial games," Physica D **75**, 292–309 (1994).

[17] M. Nakamaru, H. Matsuda, and Y. Iwasa, "The evolution of cooperation in a lattice-structured population," J. Theor. Biol. **184**, 65–81 (1997).

[18] G. Szabó and C. Tőke, "Evolutionary prisoner's dilemma game on a square lattice," Phys. Rev. E **58**, 69–73 (1998).

[19] K. Brauchli, T. Killingback, and M. Doebeli, "Evolution of cooperation in spatially structured populations," J. Theor. Biol. **200**, 405–417 (1999).

[20] E. Ising, "Beitrag zur Theorie des Ferromagnetismus," Z. Phys. **31**, 253–258 (1925).

[21] J. Nash, "The bargaining problem," Econometrica **18**, 155–162 (1950).

[22]J. Hofbauer and K. Sigmund, *Evolutionary Games and Population Dynamics* (Cambridge U. P., Cambridge, 1998).

[23]R. J. Glauber, "Time-dependent statistics of the Ising model," J. Math. Phys. **4**, 294–307 (1963).

[24]J. Marro and R. Dickman, *Nonequilibrium Phase Transitions in Lattice Models* (Cambridge U. P., Cambridge, 1999).

[25]H. Hinrichsen, "Non-equilibrium critical phenomena and phase transitions into absorbing states," Adv. Phys. **49**, 815–958 (2000).

[26]W. D. Hamilton, "The evolution of altruistic behaviour," Am. Nat. **97**, 354–356 (1963).

[27]R. Dawkins, *The Selfish Gene: New Edition* (Oxford U. P., Oxford, 1989).

[28]J. B. S. Haldane, *The Causes of Evolution* (Longman, New York, 1932).

[29]S. R. Broadbent and J. M. Hammersley, "Percolation processes, I. Crystals and mazes," Proc. Cambridge Philos. Soc. **53**, 629–645 (1957).

[30]T. E. Harris, "Contact interactions on a lattice," Ann. Prob. **2**, 969–988 (1974).

[31]D. H. Zanette, "Dynamics of rumor propagation on small-world networks," Phys. Rev. E **65**, 041908-1–9 (2002).

[32]J. L. Cardy and U. C. Täuber, "Field theory of branching and annihilating random walks," J. Stat. Phys. **90**, 1–56 (1998).

[33]A. Lipowski and M. Droz, "Phase transitions in nonequilibrium d-dimensional models with q absorbing states," Phys. Rev. E **65**, 056114-1–7 (2002).

[34]S. Milgram, "The small world problem," Psychol. Today **2**, 60–67 (1967).

[35]M. E. J. Newman, "The structure and function of complex networks," SIAM Rev. **45**, 167–256 (2003).

[36]R. Albert and A. L. Barabási, "Statistical mechanics of complex networks," Rev. Mod. Phys. **74**, 47–97 (2002).

[37]D. J. Watts and S. H. Strogatz, "Collective dynamics of 'small world' networks," Nature (London) **393**, 440–442 (1998).

[38]B. Bollobás, *Random Graphs* (Academic, New York, 1995).

[39]G. Szabó, "Branching annihilating random walk on random regular graphs," Phys. Rev. E **62**, 7474–7477 (2000).

[40]M. A. Nowak, S. Bonhoeffer, and R. M. May, "More spatial games," Int. J. Bifurcation Chaos Appl. Sci. Eng. **4**(1), 33–56 (1994).

[41]M. H. Vainstein and J. J. Arenzon, "Disordered environments in spatial games," Phys. Rev. E **64**, 051905-1–6 (2001).

[42]G. Abramson and M. Kuperman, "Social games in a social network," Phys. Rev. E **63**, 030901-1–4 (2001).

[43]B. J. Kim, A. Trusina, P. Holme, P. Minnhagen, J. S. Chung, and M. T. Choi, "Dynamic instabilities induced by asymmetric influence: Prisoner's dilemma game in small-world networks," Phys. Rev. E **66**, 021907-1–4 (2002).

[44]H. Ebel and S. Bornholdt, "Coevolutionary games on networks," Phys. Rev. E **66**, 056118-1–8 (2002).

[45]J.-J. Rousseau, *The Inequality of Man* (1755); reprinted in *Rousseau's Social Contract and Discourses*, edited by G. Cole (Dent, London, 1913), pp. 157–246.

[46]C. Hauert, S. De Monte, J. Hofbauer, and K. Sigmund, "Replicator dynamics in optional public goods games," J. Theor. Biol. **218**, 187–194 (2002).

[47]G. Szabó and C. Hauert, "Evolutionary prisoner's dilemma games with voluntary participation," Phys. Rev. E **66**, 062903-1–4 (2002).

[48]C. Hauert, "Virtuallabs: Interactive tutorials on evolutionary game theory," ⟨http://www.univie.ac.at/virtuallabs⟩.

[49]K. Tainaka, "Paradoxical effect in a three-candidate voter model," Phys. Lett. A **176**, 303–306 (1993).

[50]M. Frean and E. R. Abraham, "Rock-scissors-paper and the survival of the weakest," Proc. R. Soc. London, Ser. B **268**, 1323–1327 (2001).

[51]B. Kerr, M. A. Riley, M. W. Feldman, and B. J. M. Bohannan, "Local dispersal promotes biodiversity in a real-life game of rock-paper-scissors," Nature (London) **418**, 171–171 (2002).

[52]G. Szabó and J. Vukov, "Cooperation for volunteering and partially random partnerships," Phys. Rev. E **69**, 036107-1–7 (2004).

[53]P. Ball, *Critical Mass: How One Thing leads to Another* (Heinemann, London, 2004).

[54]G. Szabó, T. Antal, P. Szabó, and M. Droz, "Spatial evolutionary prisoner's dilemma game with three strategies and external constraints," Phys. Rev. E **62**, 1095–1103 (2000).

[55]L. Frachebourg, P. L. Krapivsky, and E. Ben-Naim, "Segregation in a one-dimensional model of interacting species," Phys. Rev. Lett. **77**, 2125–2128 (1996).

[56]G. Szabó, A. Szolnoki, and R. Izsák, "Rock-scissors-paper game on regular small-world networks," J. Phys. A **37**, 2599–2609 (2004).
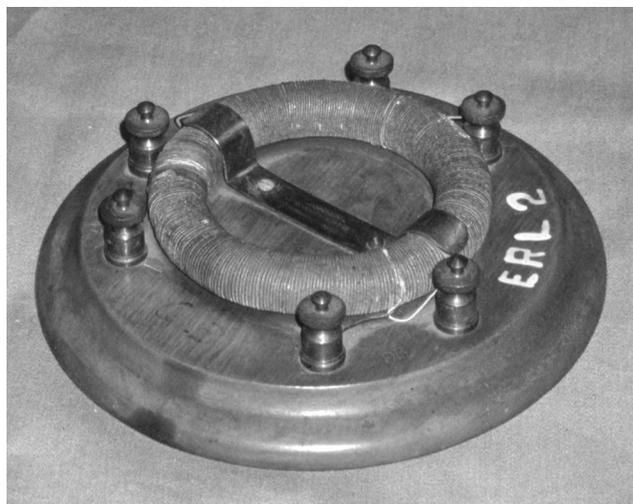
Rowland's Ring. Rowland's Ring is a device for tracing out curves of magnetic induction for an iron ring as a function of the magnetizing field applied to it. The resulting trace is known as a hysteresis curve, and the area enclosed by the B-H curve is a measure of the losses in the iron when it goes through a complete cycle. Up to the 1960s the experiment was done with aid of a ballistic galvanometer; today we would probably wind the coils on a ferrite ring and use a modern integrating circuit in place of the galvanometer. Henry Augustus Rowland (1858–1901) developed the device and experiment. This example is in the Greenslade collection. (Photograph and Notes by Thomas B. Greenslade, Jr., Kenyon College)